Alleviating effect of lycorine on CFA-induced arthritic pain via inhibition of spinal inflammation and oxidative stress

YIN-DI HU[1*], YUAN-FEN YUE[2*], TAO CHEN[2*], ZHAO-DI WANG[1], JIE-QING DING[1], MIN XIE[1], DAI LI[1], HAI-LI ZHU[1] and MENG-LIN CHENG[1]

[1]School of Pharmacy, Xianning Medical College, Hubei University of Science and Technology; [2]Department of Pharmacy, Xianning Central Hospital, First Affiliated Hospital of Hubei University of Science and Technology, Xianning, Hubei 437100, P.R. China

Received October 21, 2022; Accepted March 16, 2023

DOI: 10.3892/etm.2023.11940

Abstract. Chronic pain is the primary symptom of osteoarthritis affecting a patient's quality of life. Neuroinflammation and oxidative stress in the spinal cord contribute to arthritic pain and represent ideal targets for pain management. In the present study, a model of arthritis was established by intra-articular injection of complete Freund's adjuvant (CFA) into the left knee joint in mice. After CFA inducement, knee width and pain hypersensitivity in the mice were increased, motor disability was impaired, spinal inflammatory reaction was induced, spinal astrocytes were activated, antioxidant responses were decreased, and glycogen synthase kinase 3β (GSK-3β) activity was inhibited. To explore the potential therapeutic options for arthritic pain, lycorine was intraperitoneally injected for 3 days in the CFA mice. Lycorine treatment significantly reduced mechanical pain sensitivity, suppressed spontaneous pain, and recovered motor coordination in the CFA-induced mice. Additionally, in the spinal cord, lycorine treatment decreased the inflammatory score, reduced NOD-like receptor protein 3 inflammasome (NLRP3) activity and IL-1β expression, suppressed astrocytic activation, downregulated NF-κB levels, increased nuclear factor erythroid 2-related factor 2 expression and superoxide dismutase activity. Furthermore, lycorine was shown to bind to GSK-3β through three electrovalent bonds, to inhibit GSK-3β activity. In summary, lycorine treatment inhibited GSK-3β activity, suppressed NLRP3 inflammasome activation, increased the antioxidant response, reduced spinal inflammation, and relieved arthritic pain.

Correspondence to: Dr Hai-Li Zhu or Dr Meng-Lin Cheng, School of Pharmacy, Xianning Medical College, Hubei University of Science and Technology, 88 Xianning Avenue, Xianning, Hubei 437100, P.R. China
E-mail: hkhaili_zhu@163.com
E-mail: menglincheng@hbust.edu.cn

*Contributed equally

Key words: arthritic pain, spinal inflammation, oxidative stress, lycorine, glycogen synthase kinase 3β

Introduction

Osteoarthritis (OA) is a chronic, debilitating, and degenerative joint disease, that affects ~250 million individuals worldwide (1). Chronic pain is the primary symptom of OA, and it reduces a patient's quality of life, and is an important factor in the management of OA (2). Common pharmacological treatments for OA are acetaminophen, non-steroidal anti-inflammatory drugs, and opioids (3). Due to the uncertain efficacies and overall safety of these agents, OA pain management remains largely inadequate, it is becoming a major public health concern (4). Therefore, illustrating the mechanisms of OA pain may be useful for developing novel treatments for the management of OA pain.

Joint destruction and disability trigger numerous pain-producing agents and stimulate nociceptive signals, which are transmitted to the spinal dorsal horn and brain, and finally cause chronic pain (5). During this process, the spinal cord undergoes central sensitization, resulting in increased excitability and synaptic efficacy of neurons and activation of glial cells (6). The prevalence of central sensitization is observed in 35.3% of 150 inflammatory arthritis patients (7). Lower pain thresholds and punctate hyperalgesia in the area of concern are thus often observed in patients with OA (8). Patients with advanced OA often experience widespread pain at the OA joint and even in the whole leg (9). In an OA animal model, mechanical hyperalgesia and allodynia are also observed (5). Activated glial cells, especially astrocytes, undergo morphological changes, activating a neuroinflammatory response via the release of a variety of pro-inflammatory cytokines, stimulating nociceptive synaptic transmission, modulating pain signaling, and regulating pain maintenance (10). In spinal cord injury patients who experience neuropathic pain, the levels of metabolites that regulate neuroinflammation are elevated based on magnetic resonance spectroscopy (11). In patients suffering from a common chronic pain disorder (lumbar radiculopathy), the levels of the neuroinflammation marker 18 kDa translocator protein in the spinal cord are also elevated (12). The levels of IL-1α, IL-1β, TNF-α, IL-17, and other inflammatory mediators

are also significantly increased in the lumbar spinal cord of the OA pain rat model (13). Additionally, NF-κB expression (a transcription factor for inflammatory responses) and astrocyte proliferation are also increased in the spinal dorsal horn (14). Further, spinal inhibition of NF-κB significantly alleviates mechanical hyperalgesia and decreases the expression of the inflammatory cytokines IL-1β, TNF-α, and IL-33 in the dorsal horn of OA animals (15). Inhibition of spinal inflammation alleviates OA pain.

Oxidative stress, a result of an imbalance between the production of reactive oxygen species (ROS) and their clearance by the antioxidant defense system, is a major cause of chronic inflammation and pain (16). In the whole blood and in the monocytes of rheumatoid arthritis patients, mitochondrial ROS production is increased five-fold, compared with healthy subjects (17). Blood concentrations of a lipid oxidation biomarker, malondialdehyde (MDA), in rheumatoid arthritis patients are significantly increased (18). In an OA murine model, deletion of the transcription factor nuclear factor (erythroid-derived 2)-like 2 (Nrf2) resulted in increased OA severity (19). Additionally, oxidative stress-activated cellular signal transduction pathways, such as NF-κB inflammatory signal and the caspase signaling pathway, leading to chronic inflammation (20). In a monoarthritic rat model, injection of methane-rich saline suppressed oxidative stress (MDA and 8-OHDG), increased superoxide dismutase and catalase activity, and reduced chronic inflammatory pain (21). Thus, targeting oxidative stress may be an effective treatment for the management of spinal inflammation and OA chronic pain.

Lycorine is a pyrrolo[de]phenanthridine ring-type alkaloid isolated from the *Amaryllidaceae* family of plants that possesses anti-tumor, anti-viral, and anti-inflammatory properties (22). Lycorine works as a potent anti-tumor compound against various types of cancer cells, including gastric cancer, bladder cancer, colorectal cancer, prostate cancer, and breast cancer, amongst others (23). Lycorine is effective in a very low, single digit μM concentration and is well tolerated with minimal toxicity. In tumor xenografted mouse models, 5-15 mg/kg/day lycorine treatment did not induce any significant changes in the mice, thus being indicative of very low to no toxicity (24). Additionally, lycorine possesses significant anti-inflammatory and hepatoprotective effects on mice at doses ranging from 1-2 mg/kg, decreases the percentages of immature granular leukocytes, and may be useful in the management of acute promyelocytic leukemia at 5-10 mg/kg (25). Lycorine also has analgesic effects. In an acetic-acid and carrageenan-induced rat model of pain, lycorine intraperitoneal administration (i.p) showed antinociceptive and anti-inflammatory effects at doses of 1.0 and 1.5 mg/kg (26). In an intervertebral disc degeneration model, 5 mg/kg lycorine (i.p) inhibited NF-κB-mediated proinflammatory cytokine expression to prevent degeneration (27). In a model of pulmonary inflammation and fibrosis, lycorine inhibited NOD-like receptor protein 3 (NLRP3) inflammasome activation and pyroptosis to act as a therapeutic agent (28). In a model of cardiac dysfunction, lycorine treatment inhibited inflammation and oxidative stress in heart tissues (29). Thus, in the present study, the role and pathological mechanism of lycorine on neuroinflammation and arthritic pain were studied.

A complete Freund's adjuvant (CFA) induced arthritic pain mouse model was established, which is a commonly used model for research on chronic polyarthritis for the evaluation of the anti-inflammatory and analgesic potential of drugs (30,31). CFA inducement results in pathophysiological changes such as synovial hyperplasia and cartilage degradation, which are similar to clinical arthritis (32). Here, lycorine was intraperitoneally administered in mice, and the effects of lycorine on behavioral, morphological, and protein expression changes were analyzed. The results of the present study provide a theoretical basis for the development of lycorine as an analgesic drug for the management of arthritic pain.

Materials and methods

Animal model and drug administration. A total of 30 male C57BL/6J mice weighing 18-20 g (6-8 weeks old) were purchased from Hubei Province Experimental Animal Center. All animals were housed with a 12 h light/dark with *ad libitum* access to standard mouse chow and water. All efforts were made to minimize the number of animals used and their suffering. The toe-pinch reflex and a loss of righting reflex were used to determine the level of anesthesia in the present study (33,34). Apnea and the cessation of the heartbeat were used to confirm death (35). If mice became sick or injured, they were euthanized using an overdose (150 mg/kg) of pentobarbital sodium by intraperitoneal injection.

Mice were acclimatized to the environment for 5 days prior to the experiments, and randomly divided into three groups: Control, CFA, and CFA + lycorine (n=10 per group). A mouse model of CFA was established by intra-articular injection with 10 μl CFA into the left hind knee joint on days 0 and 7; the control group was injected with the same volume of saline (36). Behavioral tests were performed on days 0, 7, and 14. On days 15-17 after CFA injection, mice from the CFA and CFA + lycorine groups were intraperitoneally injected with vehicle or lycorine (10 mg/kg), respectively, for 3 consecutive days (37). Lycorine (Shanghai yuanye Bio-Technology) was dissolved in DMSO and diluted with 0.9% NaCl before use. Subsequently, behavioral tests were performed at 4 h after lycorine administration. Following completion of the behavioral tests, all animals were sacrificed for further experimental analysis.

Antibodies and reagents. Anti-IL-1β rabbit polyclonal antibody (cat. no. AF5103), glial fibrillary acidic protein (GFAP) rabbit polyclonal antibody (cat. no. DF6040), p-GSK3β (S9) rabbit polyclonal antibody (cat. no. AF2016), GSK3β rabbit polyclonal antibody (cat. no. AF5016), Caspase 1 rabbit polyclonal antibody (cat. no. AF5418), cleaved-Caspase 1 rabbit polyclonal antibody (cat. no. AF4005), and β-actin rabbit antibody (cat. no. AF7018) were obtained from Affinity Biosciences, Ltd. Nrf2 rabbit polyclonal antibody (cat. no. A1244), NLRP3 rabbit polyclonal antibody (cat. no. A5652), and NF-κB rabbit polyclonal antibody (cat. no. A19653) were purchased from ABclonal Biotech Co., Ltd. Hematoxylin and eosin (H&E) staining solution (cat. no. BL735B) was purchased from Biosharp Life Sciences. Lycorine was purchased from Shanghai yuanye Bio-Technology. The secondary antibody used for western blotting was an HRP Goat anti-rabbit IgG

(H+L) (cat. no. AS014, ABclonal Biotech Co., Ltd.). The secondary antibody used for immunofluorescence analysis was a Goat Anti-Rabbit IgG H&L (FITC) (cat. no. ab6717, Abcam).

Mechanical threshold test. Mechanical threshold values, which are indicative of mechanical pain sensitivity, were measured and presented as the paw withdrawal threshold (38). Von Frey filaments (Stoelting; ranging from 0.008 to 6.0 g) were used to stimulate the left hind paw. Mice were placed in a 30x30x30 cm plexiglass chamber and allowed to acclimatize for at least 30 min before the behavioral experiments were performed. Filaments were pressed vertically against the plantar surfaces until the filaments were bent and held for 3-5 sec, and a brisk withdrawal and paw flinching was considered a positive response. Once a positive response was observed, the von Frey filament with the next lower force was applied, and whenever a response was not observed, the filament with the next higher force was applied. Then, the pattern of positive and negative withdrawal responses was converted to the mechanical threshold as described previously (39).

Spontaneous flinch test. The number of flinches representative of spontaneous pain was recorded. Mice were placed in a 30x30x30 cm plexiglass chamber and acclimatized for at least 30 min. The number of flinches in 5 min was counted three times independently. The mean of the total number of flinches was taken (40).

Rotarod test. An accelerating rotarod was used to assess motor coordination and the balance of animals. Three days before the experiments, the mice were trained at a fixed speed of 4 revolutions/min for 10 min and this was repeated 3 times at 10 min intervals. At the beginning of the experiment, the rotation speed was set at a fixed value of 10 revolutions/min for 10 sec, accelerated for 10 sec to a working speed of 20 revolutions/min for 30 sec, and then accelerated again for 10 sec. This movement was continuously carried out for 10 min. Experiments were repeated three times with intervals of 10 mins. The latency to fall of rats was recorded (41).

H&E staining. After behavioral tests were performed, 5 C57BL/6J mice in each group were anesthetized using 60 mg/kg sodium pentobarbital by intraperitoneal injection, perfused transcardially with saline containing heparin, following perfusion with 4% paraformaldehyde (PFA, 0.1 M phosphate buffer, pH 7.4) until the animal body was stiff and rigid. After perfusion, spinal cords were collected and post-fixed in 4% PFA for 12 h at 4˚C, embedded in paraffin, and cut into 4 μm sections using a microtome (RM 2165; Leica Microsystems GmbH). The sections were stained using the standard H&E method. Briefly, after dewaxing, the sections were dyed with hematoxylin solution for 20 min at 25˚C and washed with tap water for 10 sec. Subsequently, the sections were stained with eosin for 5 min at 25˚C and washed with tap water for 10 sec. The dehydration and transparent treatment were conducted by placing the slices in 70% ethanol (10 sec at 25˚C), 80% ethanol (10 sec at 25˚C), 90% ethanol (30 sec at 25˚C), 100% ethanol (1 min at 25˚C) and xylene (1 min twice at 25˚C). Finally, the sections were sealed with neutral balsam and observed using a fluorescence microscope (Olympus IX73; Olympus Corporation). The images were analyzed using ImageJ version 1.51j8 (National Institutes of Health). The scoring criteria of inflammatory cell infiltration was: 0, normal; 1, lymphocyte infiltration around meninges and blood vessels; 2, 1-10 lymphocytes in a field; 3, 11-100 lymphocytes in a field of view; 4, >100 lymphocytes in a field of view.

Immunofluorescence analysis. Spinal cord sections were dewaxed, antigen retrieval was performed using Improved Citrate Antigen Retrieval Solution (cat. no. P0083, Beyotime Institute of Biotechnology) according to the manufacturer's protocol, treated with hydrogen peroxide, blocked with immunofluorescence blocking solution (Beyotime Institute of Biotechnology) at 25˚C for 1 h, incubated with a primary antibody overnight at 4˚C, and subsequently incubated with fluorescent secondary antibody at 25˚C for 1 h and observed under a fluorescence microscope (Olympus IX73; Olympus Corporation). The fluorescence intensities were analyzed using ImageJ. The following primary antibodies were used: Anti-IL-1β (1:100), anti-Nrf2 (1:100), anti-GFAP (1:100), anti-Caspase 1 (1:100), anti-p-GSK3β (S9) (1:100), and anti-NF-κB (1:100).

Western blotting. After behavioral tests, another 5 mice from each group were euthanized with an overdose of pentobarbital sodium (150 mg/kg) by intraperitoneal injection and sacrificed through decapitation. Lumbar spinal cord samples were collected, homogenized in RIPA lysis buffer containing 1% protease inhibitors (MilliporeSigma), centrifuged at 13,523 x g, 4 ˚C for 20 min. The supernatant was collected, loaded on an 8-12% SDS gel, resolved using SDS-PAGE, and transferred to PVDF membranes. Protein concentrations were quantified using a BCA protein assay kit (Beyotime Institute of Biotechnology). The membranes were blocked with QuickBlock™ Blocking Buffer for Western Blot (Beyotime Institute of Biotechnology) for 15 min at 25˚C, and incubated with the appropriate primary antibodies overnight at 4˚C, followed by HRP-conjugated secondary antibodies in TBST (1:50,000) at 25˚C for 1 h. Protein bands were visualized using Super-sensitive Enhanced Chemiluminescence Substrate Kit (Biosharp Life Sciences) and visualized using an iBright 1500 instrument (Invitrogen; Thermo Fisher Scientific, Inc.). Densitometry analysis was performed using ImageJ. β-actin was used as a loading control. The following primary antibodies were used: Anti-IL-1β (1:1,000), anti-GFAP (1:1,000), anti-NF-κB (1:1,000), anti-Cleaved-Caspase 1 (1:1,000), anti-Nrf2 (1:1,000), anti-NLRP3 (1:1,000), anti-Phospho-GSK3β (S9) (1:1,000), anti-GSK3β (1:1,000), and anti-β-actin (1:50,000).

Molecular docking. The X-ray crystal structure of GSK-3β was obtained from the Protein Data Bank (PDB ID: 2o5k, https://www.rcsb.org/). The structure of lycorine was downloaded from the PubChem database (https://www.pubchem.ncbi.nlm.nih.gov/compound) and optimized using ChemBio3D Ultra 14.0 software (PerkinElmer Informatics). Auto Dock Vina 1.2.0 software (Center for Computational Structural Biology) was used for docking conformation between GSK-3β

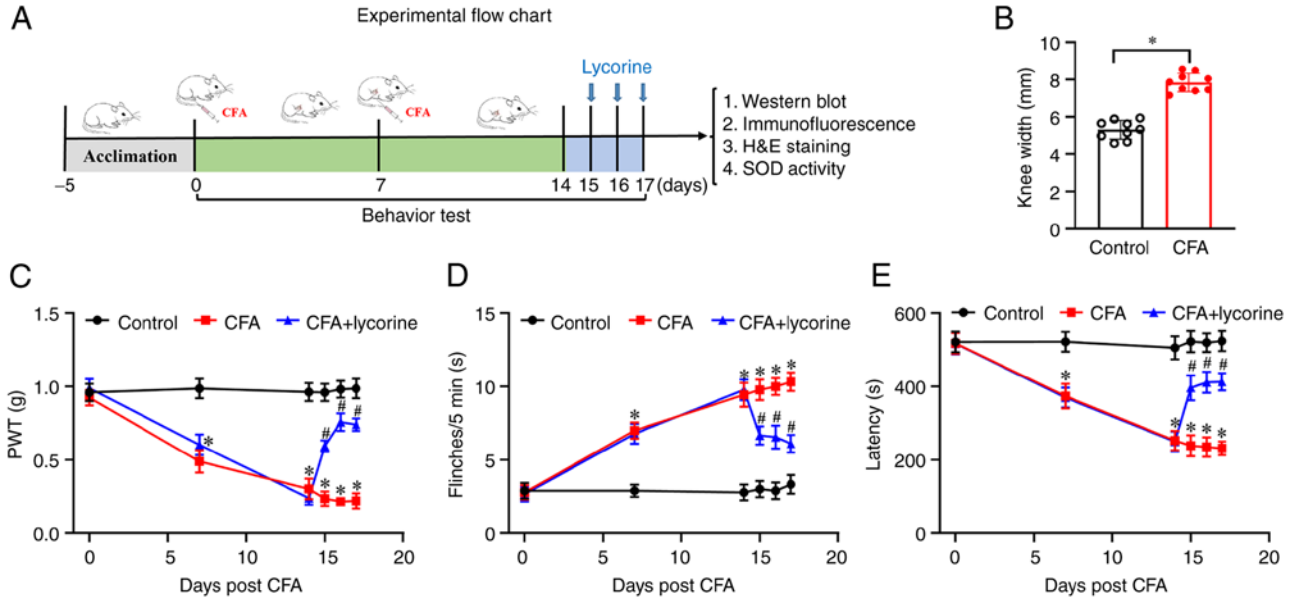

Figure 1. Effect of lycorine treatment on pain response in the CFA mice. (A) Schematic diagram of the experimental procedures. On days 0 and 7, CFA was intraarticularly injected into the left knee joint of the mice, and behavioral tests were performed on days 0, 7, and 14. Lycorine was intraperitoneally injected in mice on days 15-17; 4 h after lycorine treatment, behavioral tests were performed. Subsequently mice were sacrificed, and the spinal cord tissues were collected for further analysis. (B) Changes of knee width from control in the CFA mice on day 14 after CFA treatment. (C) Changes of PWT values, (D) spontaneous flinches, and (E) latency to fall values in the mice. Data are presented as the mean ± SEM (n=9). *P<0.05 vs. control group; #P<0.05 vs. CFA group. CFA, complete Freund's adjuvant; PWT, paw withdrawal threshold; SOD, superoxide dismutase.

and lycorine. PyMOL version 2.2.3 (DeLano Scientific) was used to visualize the conformation.

Measurement of superoxide dismutase (SOD) activity. For the determination of SOD enzyme activity, the CuZn/Mn-SOD assay kit with WST-8 (cat. no. S0103; Beyotime Institute of Biotechnology) was used. Briefly, spinal cords were homogenized in ice-cold PBS buffer, centrifuged at 13,523 x g at 4˚C for 15 min, and the supernatant was collected and mixed with WST-8 enzyme working solution for 20 min at 37˚C, the OD_{450nm} absorbance value of each well was measured. SOD activity was expressed as units per mg of total protein (U/mg protein).

Statistical analysis. All statistical analysis was performed using SPSS 21.0 statistics software (IBM Corp.). A paired samples t-test was used to compare the means of knee width. A one-way ANOVA followed by Tukey's post-hoc test was used to analyze the data for behaviors, H&E staining, immunofluorescence analysis, and western blotting. Data for behavioral tests are presented as the mean ± SEM. Data for H&E staining, immunofluorescence, and western blotting are presented as the mean ± SD. P<0.05 was considered to indicate a statistically significant difference.

Results

Lycorine treatment relieves pain hypersensitivity in the CFA mice. Behavioral tests were performed using the protocol shown in Fig. 1A. As shown in Fig. 1B, on day 14, CFA treatment led to a swelling of the knee. The knee width of the mice in the control group was 5.32±0.17 mm, while in the CFA group, it was 7.85±0.17 mm (P<0.05). Additionally, compared with the control group, mechanical threshold values were significantly lower in the CFA mice from 0.92±0.05 (day 0) to 0.49±0.08 (day 7, P<0.05), 0.30±0.07 (day 14, P<0.05) (Fig. 1C). The number of flinches was significantly increased in the CFA mice from 2.78±0.49 (day 0) to 7±0.55 (day 7, P<0.05), 9.44±0.82 (day 14, P<0.05) (Fig. 1D). Latency to fall was reduced in the CFA mice from 518.34±28.34 (day 0) to 374.23±33.36 (day 7, P<0.05), and 252.91±26.48 (day 14, P<0.05) (Fig. 1E). These data showed that CFA treatment-induced pain hypersensitivity and motor disability in the mice; that is, the mouse model of arthritis had been successfully established. The effect of lycorine on pain sensitivity and motor ability was next assessed. After lycorine treatment on days 15-17, mechanical threshold values of CFA + lycorine mice were significantly higher, 0.59±0.04, 0.76±0.06, and 0.74±0.04 on days 15-17, respectively (P<0.05 vs. CFA group) (Fig. 1C). The number of flinches in the CFA + lycorine mice was notably lower, 6.67±0.62, 6.56±0.78, and 6.11±0.61, on days 15-17, respectively (P<0.05 vs. CFA group) (Fig. 1D). The latency to fall of CFA + lycorine mice were increased to 396.97±34.35, 411.65±28.43 and 413.21±23.69, on days 15-17, respectively (P<0.05 vs. CFA group) (Fig. 1E). Thus, lycorine treatment increased mechanical pain sensitivity, suppressed spontaneous pain, and promoted recovery of motor coordination in the CFA-induced mice.

Lycorine treatment decreases spinal inflammation. Spinal inflammatory reactions were determined based on inflammatory infiltration and IL-1β expression levels. Using H&E staining, infiltration of inflammatory cells was increased in the spinal dorsal horn of the CFA mice with the relative inflammation score at 2.80±0.14. (P<0.05 vs. control group, Fig. 2A); lycorine treatment decreased the inflammatory response

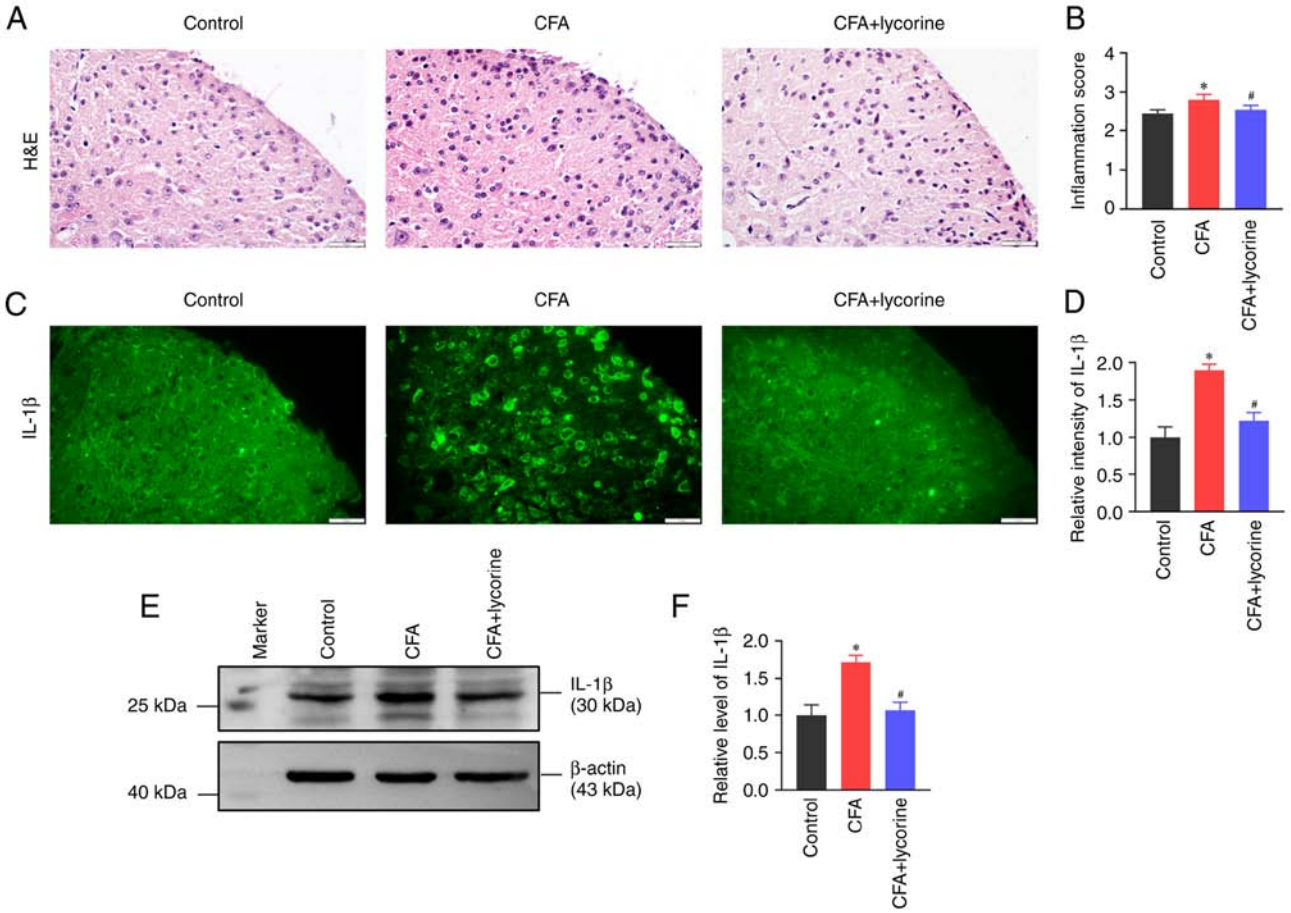

Figure 2. Effect of lycorine treatment on spinal inflammatory infiltration and IL-1β expression. (A) Representative H&E-stained images of spinal cord sections from the control, CFA and CFA + lycorine groups. Scale bar, 20 μm. (B) Quantitative analysis of inflammation score of the H&E staining in each group. Representative immunofluorescence staining images of (C) IL-1β expressions in spinal dorsal horn and (D) quantitative fluorescence intensity analysis. Scale bar, 20 μm. (E) Representative western blots and (F) densitometry analysis of IL-1β expression levels in the spinal cords of the control, CFA, and CFA + lycorine groups. Data are presented as the mean ± SD (n=5). *P<0.05 vs. control group; #P<0.05 vs. CFA group. CFA, complete Freund's adjuvant; H&E, hematoxylin and eosin.

with a relative inflammation score of 2.55±0.12 (P<0.05 vs. CFA group, Fig. 2B). Meanwhile the expression levels of IL-1β were detected using immunofluorescence staining and western blotting. Compared with the control group, the fluorescence intensity of IL-1β in the spinal dorsal horn was significantly higher in the CFA group (P<0.05), and lycorine treatment decreased IL-1β intensity (P<0.05 vs. CFA group) (Fig. 2C). Relative intensity values of IL-1β in the CFA and CFA + lycorine groups were 1.89±0.08 and 1.22±0.11, respectively (Fig. 2D). Western blotting showed that the expression levels of spinal cord IL-1β in the CFA mice were increased to 1.71±0.09 (P<0.05 vs. control group). Lycorine treatment reduced IL-1β expression levels to 1.06±0.11 (P<0.05 vs. CFA group) (Fig. 2E and F).

Lycorine treatment suppresses spinal astrocytic activation. Astrocytic activation is an important source of inflammatory cytokines and is assessed based on GFAP levels, which is used as a marker of abnormal astrocyte activation and proliferation (42). The intensity of GFAP in the spinal dorsal horn of the CFA group was significantly increased to 1.53±0.09 (P<0.05 vs. control group), and lycorine treatment decreased the intensity to 1.10±0.11 (P<0.05 vs. CFA) (Fig. 3A and B). Consistently, spinal GFAP expression in the CFA group was increased (P<0.05 vs. control group), and this was reversed by lycorine treatment (P<0.05 vs. CFA group) (Fig. 3C). Relative gray values of GFAP in the CFA and CFA + lycorine groups were 1.60±0.12 and 1.01±0.12, respectively (Fig. 3D).

Lycorine treatment inhibits spinal NLPR3 inflammasome activity. NLRP3 inflammasome mediates Caspase 1 activation and IL-1β secretion (43). The fluorescence intensity of Caspase 1 in the spinal dorsal horn was increased in the CFA group with a relative intensity value of 1.50±0.12 (P<0.05 vs. control group). Lycorine treatment reduced the intensity of Caspase 1 to 1.03±0.09 (P<0.05 vs. CFA group) (Fig. 4A and B). Western blotting showed that spinal expression of NLRP3 and Cleaved-Caspase 1 were increased in the CFA group (P<0.05 vs. control group; Fig. 4C), and the relative grey values were 1.44±0.13 and 1.68±0.11, respectively. Lycorine treatment decreased the expression levels of NLRP3 and Caspase 1 to 1.00±0.12 and 1.03±0.06, respectively (P<0.05 vs. CFA group; Fig. 4D).

Lycorine treatment decreases spinal NF-κB levels. Distribution and expression of NF-κB in the spinal cord were

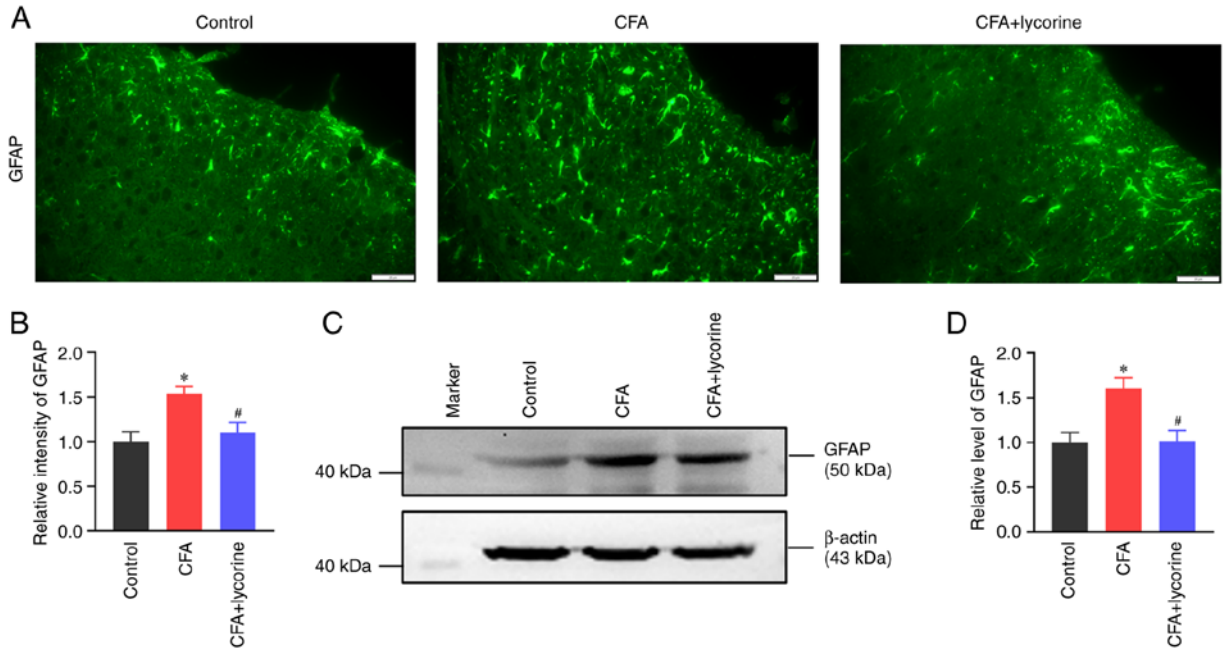

Figure 3. Effect of lycorine treatment on GFAP expression. (A) Representative immunofluorescence staining images of spinal GFAP expression in the control, CFA, and CFA + lycorine groups. Scale bar, 20 μm. (B) Quantitative analysis of fluorescence intensity of GFAP. (C) Representative western blots and (D) densitometry analysis of GFAP expression levels in the spinal cords of the control, CFA, and CFA + lycorine groups. β-actin was used as the loading control. Data are presented as the mean ± SD (n=5). *P<0.05 vs. control group, #P<0.05 vs. CFA group. CFA, complete Freund's adjuvant; GFAP, glial fibrillary acidic protein.

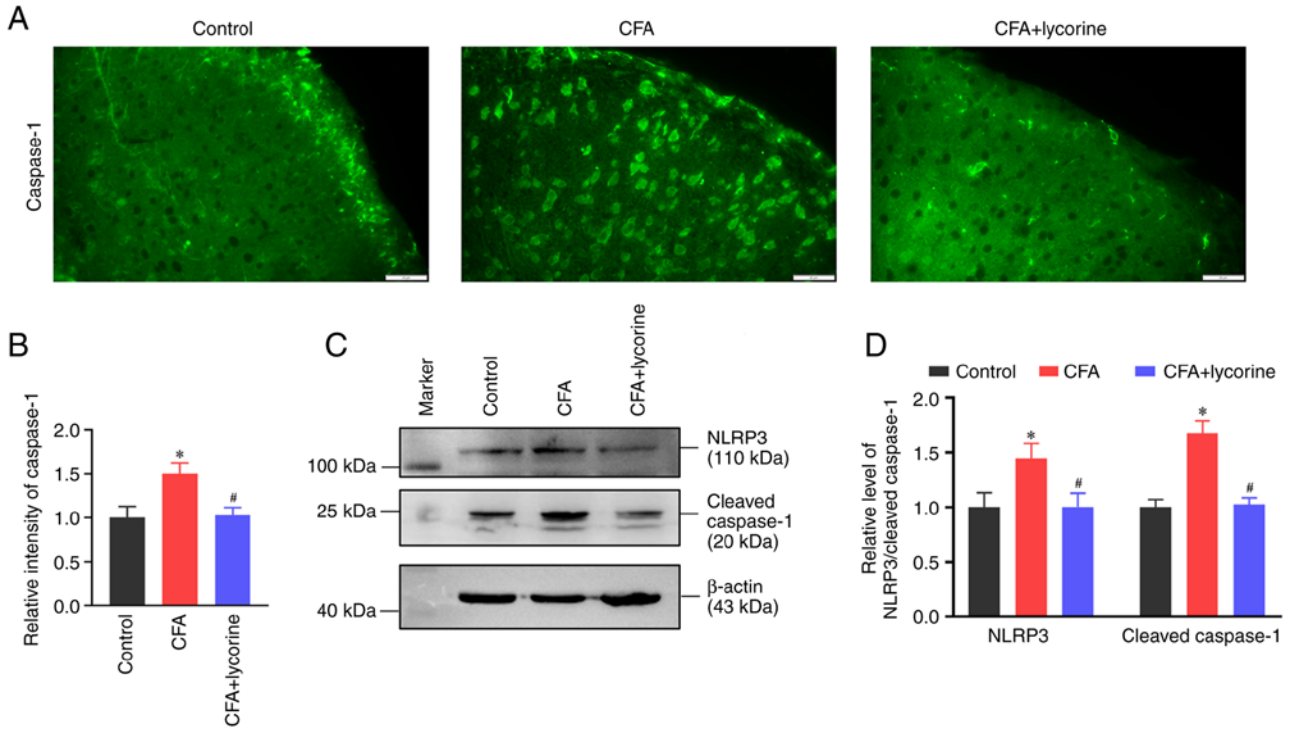

Figure 4. Effect of lycorine treatment on NLRP3 inflammasome components. (A) Representative immunofluorescence staining images and (B) quantitative analysis of spinal Caspase 1 expression levels in the control, CFA, and CFA + lycorine groups. Scale bar, 20 μm. (C) Representative western blots and (D) densitometry analysis of NLRP3 and Caspase 1 expression levels the in spinal cords of the control, CFA, and CFA + lycorine groups. β-actin was used as the loading control. Data are presented as the mean ± SD (n=5). *P<0.05 vs. control group, #P<0.05 vs. CFA group. NLRP3, NOD-like receptor protein 3 inflammasome; CFA, complete Freund's adjuvant.

analyzed. The fluorescence intensity of NF-κB in the spinal dorsal horn in the CFA group was significantly increased to 1.75±0.13 (P<0.05 vs. control group), and lycorine treatment significantly reduced the intensity to 1.20±0.09 (P<0.05 vs. CFA group) (Fig. 5A and B). NF-κB expression levels in the spinal cord was increased in the CFA group with a grey value

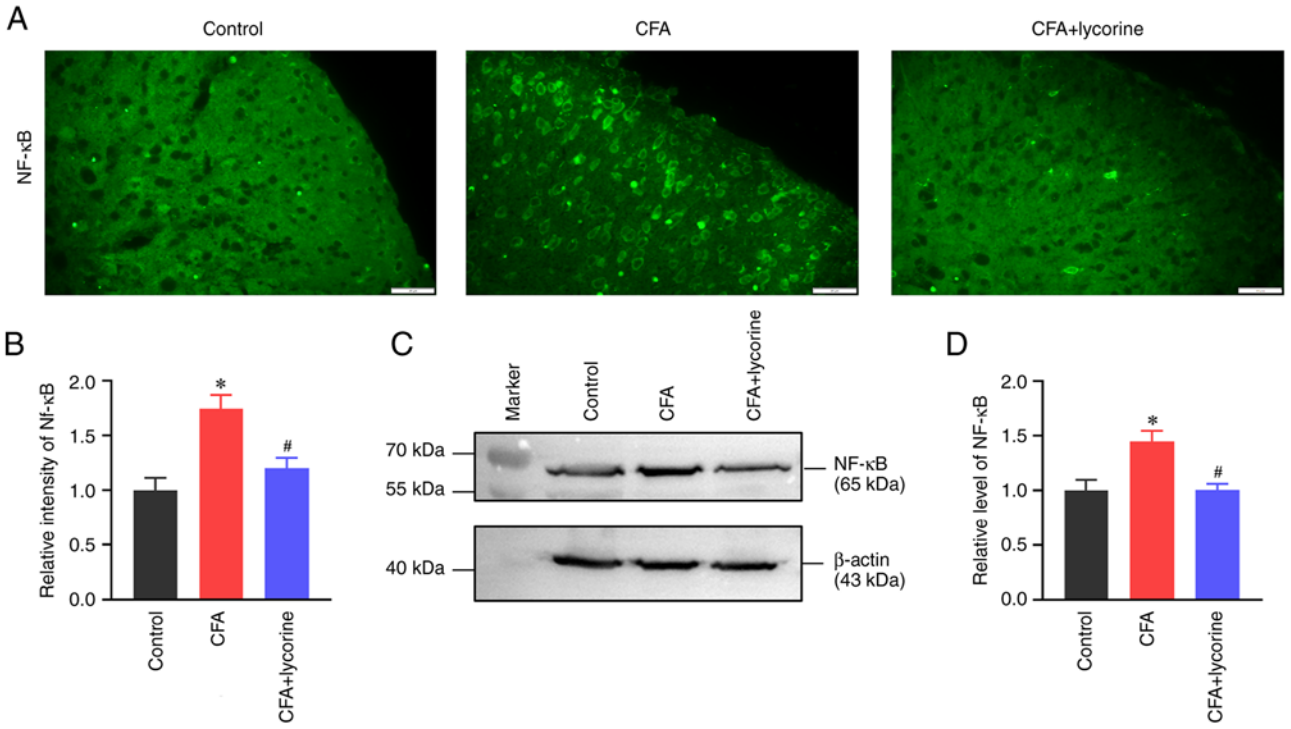

Figure 5. Effect of lycorine treatment on NF-κB expression. (A) Representative immunofluorescence stained images and (B) quantitative analysis of spinal NF-κB expression in the control, CFA, and CFA + lycorine groups. Scale bar, 20 μm. (C) Representative western blots and (D) densitometry analysis of NF-κB expression levels in the spinal cords of the control, CFA, and CFA + lycorine groups. β-actin was used as the loading control. Data are presented as the mean ± SD (n=5). *P<0.05 vs. control group, #P<0.05 vs. CFA group. CFA, complete Freund's adjuvant.

of 1.45±0.10 (P<0.05 vs. control group), and lycorine treatment significantly reduced the grey value of spinal NF-κB expression to 1.00±0.06 in the CFA + lycorine group (P<0.05 vs. CFA group) (Fig. 5C and D).

Lycorine treatment increases spinal Nrf2 expression and SOD activity. Oxidative stress was determined based on the levels of the antioxidant element Nrf2 and SOD activity. As shown in Fig. 6A, the fluorescence intensity of Nrf2 in the spinal dorsal horn was reduced in the CFA group, with a relative intensity of 0.70±0.09 (P<0.05 vs. control group). Lycorine treatment increased the intensity of Nrf2 to 0.89±0.10 (P<0.05 vs. CFA group) (Fig. 6B). Western blot analysis showed that the spinal expression of Nrf2 was reduced in the CFA group (P<0.05 vs. control group; Fig. 6C), with a relative grey value of 0.67±0.08. Lycorine treatment increased the expression levels of Nrf2 to 0.90±0.06 (P<0.05 vs. CFA group; Fig. 6D).

SOD is important in controlling ROS levels and is a significant inducer of Nrf2 (44). As shown in Fig. 6E, SOD activity in the control group was 15.06±0.98 U/mg. However, CFA treatment suppressed spinal SOD activity to 8.92±0.65 U/mg (P<0.05 vs. control group) and lycorine treatment increased the activity to 11.72±0.94 U/mg (P<0.05 vs. CFA group).

Lycorine treatment inhibits spinal GSK-3β activity. A molecular docking assay was performed on the X-ray crystal structures of GSK-3β and the ligand lycorine (Fig. 7A-C); lycorine formed three electrovalent bonds with GSK-3β at residues I85 and R141. The electrovalent bond distances were measured to be 2.3 and 2.6 angstroms between the R141 residue and the lycorine, and 2.5 angstroms between the I62 residue and the lycorine. The binding affinity was -7.0 kcal/mol.

Phosphorylation of GSK-3β at Ser-9 (p-GSK-3β-S9) represents an inactive state of GSK-3β (45). The fluorescence intensity of p-GSK-3β-S9 was lower in the spinal dorsal horn of the CFA group, with a relative fluorescence intensity of 0.59±0.06 (P<0.05 vs. control group). Lycorine treatment increased the intensity to 0.88±0.10 in the CFA + lycorine group (P<0.05 vs. CFA group) (Fig. 7D and E). Western blot analysis showed that p-GSK-3β-S9 levels were reduced in the CFA group (Fig. 7F), with a relative gray value of 0.58±0.10 (P<0.05 vs. control group; Fig. 7G). The p-GSK-3β-S9 expression was increased following lycorine treatment in the CFA + lycorine group (Fig. 7F), with a relative gray value of 0.94±0.13 (P<0.05 vs. CFA group; Fig. 7G).

Discussion

In the present study, it was found that lycorine inhibited GSK-3β activity and alleviated CFA-induced arthritic pain. GSK-3β is a potential target for pain management (46,47). In the rat model of spinal nerve ligation, mechanical allodynia and thermal hyperalgesia were increased, and GSK-3β activity was also increased (47). Additionally, the GSK-3β selective inhibitor AR-A014418 or Thiadiazolidinone-8 (TDZD-8) administration decreased mechanical allodynia (48). In a neuropathic pain rat model of chronic sciatic nerve constriction injury, intrathecal injection of ghrelin suppressed the activation of GSK-3β in the spinal dorsal horn and markedly alleviated neuropathic pain (49). In a rat model of cancer-induced bone pain, injection of the GSK-3β

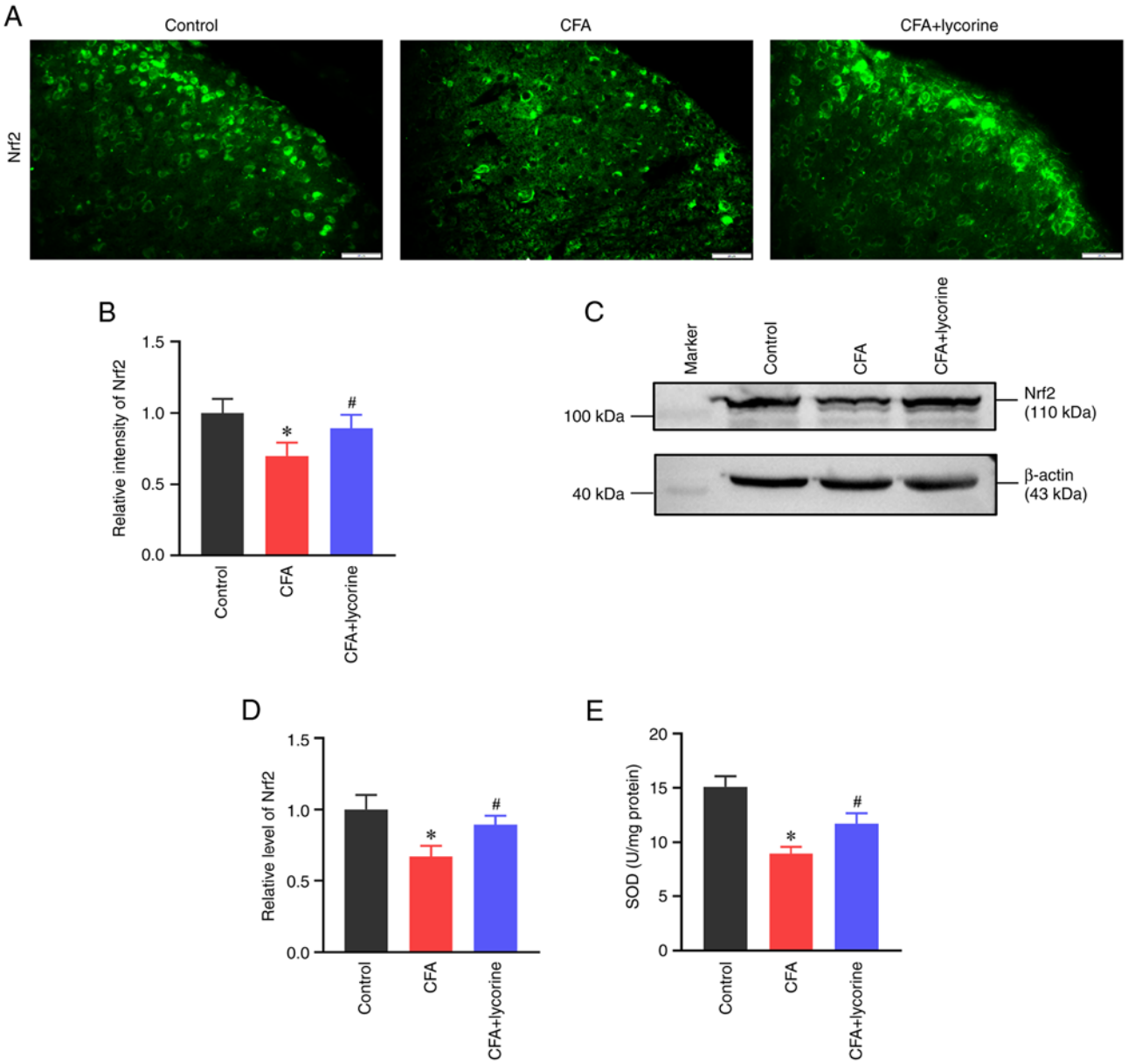

Figure 6. Effect of lycorine treatment on oxidative stress. (A) Representative immunofluorescence staining images and (B) quantitative intensity analysis of Nrf2 in the spinal dorsal horns of the control, CFA, and CFA + lycorine groups. Scale bar, 20 μm. (C) Representative western blots and (D) and densitometry analysis of the Nrf2 expression levels in the spinal cords of the control, CFA, and CFA + lycorine groups. β-actin was used as the loading control. (E) Assay for SOD activity in the spinal cord of the control, CFA, and CFA + lycorine groups. Data are presented as the mean ± SD (n=5). *P<0.05 vs. control group, $^{\#}$P<0.05 vs. CFA group. CFA, complete Freund's adjuvant; SOD, superoxide dismutase; Nrf2, nuclear factor (erythroid-derived 2)-like 2.

inhibitor TDZD-8 suppressed the NLRP3 inflammasome cascade and consequently decreased mechanical pain sensitivity (50). In a model of knee OA, pharmacological inhibitors of the GSK-3β/β-catenin pathway attenuated apoptosis (51). In the present study, GSK-3β activity was increased in the spinal cord of the CFA-induced mouse model of arthritis. Lycorine binds to the I85 and R141 residues of GSK-3β, which belong to the ATP-binding pocket and are known targets for kinase inhibitors (52). Additionally, the binding affinity between lycorine and GSK-3β was -7.0 kcal/mol, indicative of a relatively stable docking result (53). Meanwhile, GSK-3β activity was inhibited by lycorine in the spinal cord of CFA mice. Thus, the results suggested that lycorine alleviated arthritic pain by binding with GSK-3β and inhibiting its activity.

Lycorine suppressed neuroinflammation and oxidative stress in the spinal cord via the GSK-3β pathway. NF-κB serves as a pivotal mediator of inflammatory responses via inducing the expression of various pro-inflammatory genes, such as cytokines and chemokines, and by also participating in NLRP3 inflammasome regulation (54). In a model of inflammatory pain, intrathecal pretreatment with NF-κB inhibitors, namely, NF-κB decoy or pyrrolidine dithiocarbamate, reduced mechanical allodynia, and thermal hyperalgesia (55). Lycorine inhibited NF-κB signaling activity, IκB-α phosphorylation/degradation and p65 phosphorylation in prostate cancer cells and a mouse model (56). Lycorine decreased the levels of inflammatory cytokines and MDA levels by attenuating the activity of the high-mobility group box 1/Toll-like receptors/NF-κB pathway in a model of lung injury that utilizes

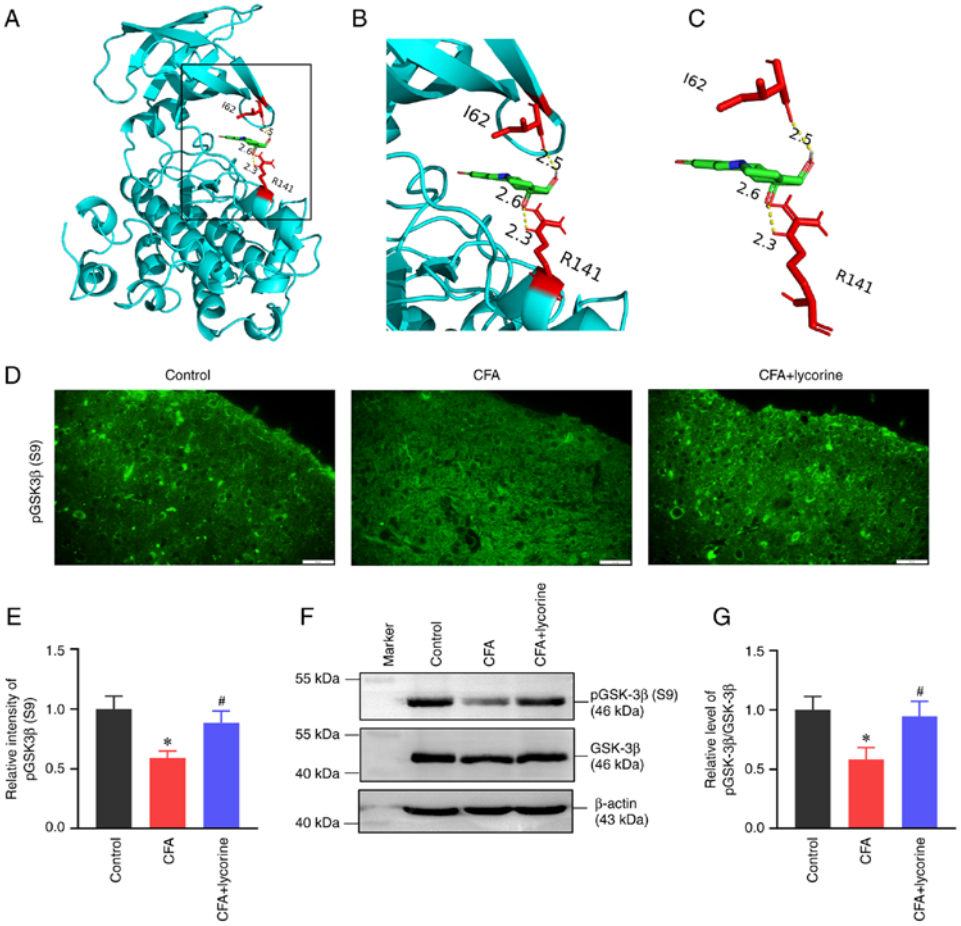

Figure 7. Effect of lycorine treatment on GSK-3β activity. (A-C) The docking results of lycorine with GSK-3β. (A) The modelled 3D structure of GSK-3β docked with lycorine. (B) Enlarged view of the binding site is shown in the inset box. (C) The interaction bonds of GSK-3β with lycorine. The GSK-3β protein is shown in cyan, lycorine is colored green, the interacting residues as red, and bonds are shown as yellow dotted lines, with bond lengths presented as numbers. (D) Representative immunofluorescence staining images and (E) quantitative intensity analysis of p-GSK-3β(S9) in the spinal dorsal horns of the control, CFA, and CFA + lycorine groups. Scale bar, 20 μm. (F) Representative western blots and (G) densitometry analysis of p-GSK-3β(S9) expression levels in the spinal cord. β-actin was used as a loading control. Data are presented as the mean ± SD (n=5). *P<0.05 vs. control group, $^{\#}$P<0.05 vs. CFA group. CFA, complete Freund's adjuvant; GSK-3β, glycogen synthase kinase 3β.

LPS (57). Lycorine also alleviated oxidative stress by reducing total reactive oxygen species, based on the lower MDA levels and higher SOD activity, significantly reduced the levels of the inflammatory cytokines IL-1β, IL-6, and TNF-α, and protected against cardiac dysfunction in a model of cardiac dysfunction (29). In the present study, it was found that lycorine reduced spinal inflammation and increased antioxidant reactions in the spinal cords of CFA model animals. Moreover, GSK-3β controls NF-κB recruitment and regulates gene transcription. GSK-3β null cells or cells treated with a GSK-3β pharmacological inhibitor exhibited reduced NF-κB DNA binding activity (58). GSK-3β also modulates the phosphorylation of the NF-κB essential modifier NEMO at serine residues 8, 17, 31 and 43, and decreases NF-κB signaling (59). Moreover, GSK-3β serves a critical role in regulating and degrading Nrf2. In liver cancer cells, inhibiting GSK-3β reduced nuclear export and degradation of Nrf2 (60). In brain ischemia and reperfusion injury, GSK-3β downregulated the expression levels of Nrf2 and its downstream genes (61). Based on the results of the present study, it was shown that lycorine suppressed NF-κB mediated spinal inflammation and enhanced the Nrf2-mediated antioxidant response via inhibition of GSK-3β activity (Fig. 8).

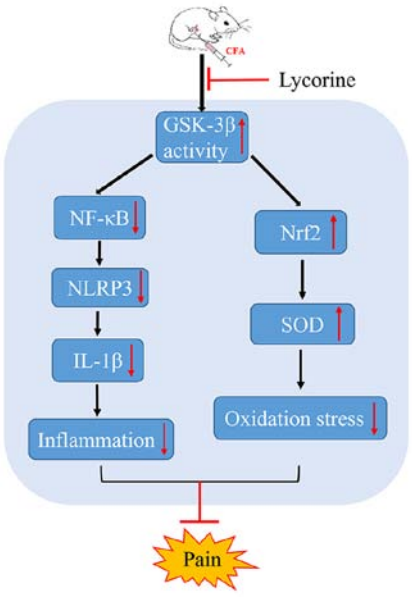

Figure 8. Schematic representation of the potential mechanism by which lycorine treatment alleviates arthritic pain. CFA, complete Freund's adjuvant; GSK-3β, glycogen synthase kinase 3β; Nrf2, nuclear factor (erythroid-derived 2)-like 2; NLRP3, NOD-like receptor protein 3 inflammasome.

The present study has some potential limitations. First, central sensitization was assessed by specific experimental proxies, such as widespread hyperalgesia, temporal summation, and descending inhibition (62). In OA pain processing, the spinal cord and brain undergo central nervous sensitization (63,64). In the present study, only the changes in the spinal cord and pain-related behaviors were detected; the changes in the brain and descending pain-modulated pathways were not analyzed. Secondly, the anti-inflammatory and pain-relief effects of lycorine on the CFA model were estimated based on three consecutive days of treatment. However, the long-term effects of lycorine and its effects (if any) on the affected joints are still not known. Finally, in this study, only the status of spinal astrocytes was evaluated; however, the microglia in the spinal cord also respond to injury and undergo rapid proliferation. Thus, the functions of microglia in OA pain should be assessed in the future. Of note, reactive astrocytes are observed in different animal models of pain, but here a focus was placed on the CFA mice. Thus, additional models should be evaluated to elaborate the astrocyte-mediated central inflammatory mechanisms.

In conclusion, during the processing of pain in OA, spinal inflammatory reactions are stimulated, spinal oxidative stress is increased, and neuropathic pain is induced. Lycorine treatment inhibits spinal GSK-3β activity, suppresses spinal NF-κB mediated inflammatory reactions, enhances spinal Nrf2-mediated antioxidant responses, and alleviates arthritic pain. Additionally, a preliminary mechanism by which lycorine alleviated neuropathic pain was determined. These results highlight the potential analgesic value of lycorine for the management of pain in patients with OA.

Acknowledgements

Not applicable.

Funding

This study was supported by grants from the National Natural Science Foundation of China (grant nos. 81971066 and 81901149), and Hubei University of Science and Technology Program (grant nos. 2020TD02 and 2020XZ40).

Availability of data and materials

The datasets used and/or analyzed during the current study are available from the corresponding author on reasonable request.

Authors' contributions

HLZ and MLC conceived and designed the study. YDH, YFY, TC, ZDW, JQD, MX, DL and HLZ acquired, analyzed and interpreted the data. YDH drafted and edited the manuscript. All authors revised the manuscript. YDH, YFY, TC, HLZ and MLC confirm the authenticity of all the raw data generated during the study. All authors have read and approved the final manuscript.

Ethics approval and consent to participate

All experimental procedures were performed according to the local and international guidelines on the ethical use of animals, and all efforts were made to minimize the number of animals used and their suffering. Ethics approval was obtained from the Laboratory Animal Ethics Committee of Hubei University of Science and Technology (approval no. 2021-05-981; Xianning, China).

Patient consent for publication

Not applicable.

Competing interests

The authors declare that they have no competing interests.

References

1. Xie SH, Wang Q, Wang LQ, Wang L, Song KP and He CQ: Effect of internet-based rehabilitation programs on improvement of pain and physical function in patients with knee osteoarthritis: Systematic review and meta-analysis of randomized controlled trials. J Med Internet Res 23: e21542, 2021.
2. Malfait AM, Miller RE and Miller RJ: Basic Mechanisms of pain in osteoarthritis: Experimental observations and new perspectives. Rheum Dis Clin North Am 47: 165-180, 2021.
3. Rajamäki TJ Jr, Puolakka PA, Hietaharju A, Moilanen T and Jämsen E: Use of prescription analgesic drugs before and after hip or knee replacement in patients with osteoarthritis. BMC Musculoskelet Disord 20: 427, 2019.
4. D'Arcy Y, Mantyh P, Yaksh T, Donevan S, Hall J, Sadrarhami M and Viktrup L: Treating osteoarthritis pain: Mechanisms of action of acetaminophen, nonsteroidal anti-inflammatory drugs, opioids, and nerve growth factor antibodies. Postgrad Med 133: 879-894, 2021.
5. Schaible HG, König C and Ebersberger A: Spinal pain processing in arthritis: Neuron and glia (inter)actions. J Neurochem: Dec 15, 2022 (Epub ahead of print).
6. Leuchtweis J, Segond von Banchet G, Eitner A, Ebbinghaus M and Schaible HG: Pain-related behaviors associated with persistence of mechanical hyperalgesia after antigen-induced arthritis in rats. Pain 161: 1571-1583, 2020.
7. Adami G, Gerratana E, Atzeni F, Benini C, Vantaggiato E, Rotta D, Idolazzi L, Rossini M, Gatti D and Fassio A: Is central sensitization an important determinant of functional disability in patients with chronic inflammatory arthritides? Ther Adv Musculoskelet Dis 13: 1759720X21993252, 2021.
8. Woolf CJ: Central sensitization: Implications for the diagnosis and treatment of pain. Pain 152 (Suppl 3): S2-S15, 2011.
9. Amodeo G, Franchi S, Galimberti G, Comi L, D'Agnelli S, Baciarello M, Bignami EG and Sacerdote P: Osteoarthritis pain in old mice aggravates neuroinflammation and frailty: The positive effect of morphine treatment. Biomedicines 10: 2847, 2022.
10. Kwon HS and Koh SH: Neuroinflammation in neurodegenerative disorders: The roles of microglia and astrocytes. Transl Neurodegener 9: 42, 2020.
11. Pfyffer D, Wyss PO, Huber E, Curt A, Henning A and Freund P: Metabolites of neuroinflammation relate to neuropathic pain after spinal cord injury. Neurology 95: e805-e814, 2020.
12. Albrecht DS, Ahmed SU, Kettner NW, Borra RJH, Cohen-Adad J, Deng H, Houle TT, Opalacz A, Roth SA, Melo MFV, *et al*: Neuroinflammation of the spinal cord and nerve roots in chronic radicular pain patients. Pain 159: 968-977, 2018.
13. Im HJ, Kim JS, Li X, Kotwal N, Sumner DR, van Wijnen AJ, Davis FJ, Yan D, Levine B, Henry JL, *et al*: Alteration of sensory neurons and spinal response to an experimental osteoarthritis pain model. Arthritis Rheum 62: 2995-3005, 2010.
14. Matsushita T, Otani K, Oto Y, Takahashi Y, Kurosaka D and Kato F: Sustained microglial activation in the area postrema of collagen-induced arthritis mice. Arthritis Res Ther 23: 273, 2021.

15. Li Y, Yang Y, Guo J, Guo X, Feng Z and Zhao X: Spinal NF-kB upregulation contributes to hyperalgesia in a rat model of advanced osteoarthritis. Mol Pain 16: 1744806920905691, 2020.
16. Ansari MY, Ahmad N and Haqqi TM: Oxidative stress and inflammation in osteoarthritis pathogenesis: Role of polyphenols. Biomed Pharmacother 129: 110452, 2020.
17. Quiñonez-Flores CM, González-Chávez SA, Del Río Nájera D and Pacheco-Tena C: Oxidative stress relevance in the pathogenesis of the rheumatoid arthritis: A systematic review. Biomed Res Int 2016: 6097417, 2016.
18. Ediz L, Hiz O, Ozkol H, Gulcu E, Toprak M and Ceylan MF: Relationship between anti-CCP antibodies and oxidant and anti-oxidant activity in patients with rheumatoid arthritis. Int J Med Sci 8: 139-147, 2011.
19. Poulet B and Beier F: Targeting oxidative stress to reduce osteoarthritis. Arthritis Res Ther 18: 32, 2016.
20. Chen L, Tian Q, Shi Z, Qiu Y, Lu Q and Liu C: Melatonin alleviates cardiac function in sepsis-caused myocarditis via maintenance of mitochondrial function. Front Nutr 8: 754235, 2021.
21. Dong D, Wu J, Sheng L, Gong X, Zhang Z and Yu C: FUNDC1 induces apoptosis and autophagy under oxidative stress via PI3K/Akt/mTOR pathway in cataract lens cells. Curr Eye Res 47: 547-554, 2022.
22. Shen J, Zhang T, Cheng Z, Zhu N, Wang H, Lin L, Wang Z, Yi H and Hu M: Lycorine inhibits glioblastoma multiforme growth through EGFR suppression. J Exp Clin Cancer Res 37: 157, 2018.
23. Xiao H, Xu X, Du L, Li X, Zhao H, Wang Z, Zhao L, Yang Z, Zhang S, Yang Y and Wang C: Lycorine and organ protection: Review of its potential effects and molecular mechanisms. Phytomedicine 104: 154266, 2022.
24. Roy M, Liang L, Xiao X, Feng P, Ye M and Liu J: Lycorine: A prospective natural lead for anticancer drug discovery. Biomed Pharmacother 107: 615-624, 2018.
25. Liu J, Li Y, Tang LJ, Zhang GP and Hu WX: Treatment of lycorine on SCID mice model with human APL cells. Biomed Pharmacother 61: 229-234, 2007.
26. Çitoğlu GS, Acikara OB, Yilmaz BS and Ozbek H: Evaluation of analgesic, anti-inflammatory and hepatoprotective effects of lycorine from Sternbergia fisheriana (Herbert) Rupr. Fitoterapia 83: 81-87, 2012.
27. Wang G, Huang K, Dong Y, Chen S, Zhang J, Wang J, Xie Z, Lin X, Fang X and Fan S: Lycorine suppresses endplate-chondrocyte degeneration and prevents intervertebral disc degeneration by inhibiting NF-κB signalling pathway. Cell Physiol Biochem 45: 1252-1269, 2018.
28. Liang Q, Cai W, Zhao Y, Xu H, Tang H, Chen D, Qian F and Sun L: Lycorine ameliorates bleomycin-induced pulmonary fibrosis via inhibiting NLRP3 inflammasome activation and pyroptosis. Pharmacol Res 158: 104884, 2020.
29. Wu J, Fu Y, Wu YX, Wu ZX, Wang ZH and Li P: Lycorine ameliorates isoproterenol-induced cardiac dysfunction mainly via inhibiting inflammation, fibrosis, oxidative stress and apoptosis. Bioengineered 12: 5583-5594, 2021.
30. Parvathy SS and Masocha W: Gait analysis of C57BL/6 mice with complete Freund's adjuvant-induced arthritis using the CatWalk system. BMC Musculoskelet Disord 14: 14, 2013.
31. Chen S, Gu Y, Dai Q, He Y and Wang J: Spinal miR-34a regulates inflammatory pain by targeting SIRT1 in complete Freund's adjuvant mice. Biochem Biophys Res Commun 516: 1196-1203, 2019.
32. Kumar VL and Roy S: Calotropis procera latex extract affords protection against inflammation and oxidative stress in Freund's complete adjuvant-induced monoarthritis in rats. Mediators Inflamm 2007: 47523, 2007.
33. Xu SF, Du GH, Abulikim K, Cao P and Tan HB: Verification and defined dosage of sodium pentobarbital for a urodynamic study in the possibility of survival experiments in female rat. Biomed Res Int 2020: 6109497, 2020.
34. Laferriere CA, Leung VS and Pang DS: Evaluating intrahepatic and intraperitoneal sodium pentobarbital or ethanol for mouse euthanasia. J Am Assoc Lab Anim Sci 59: 264-268, 2020.
35. Zatroch KK, Knight CG, Reimer JN and Pang DS: Refinement of intraperitoneal injection of sodium pentobarbital for euthanasia in laboratory rats (Rattus norvegicus). BMC Vet Res 13: 60, 2017.
36. Robledo-González LE, Martínez-Martínez A, Vargas-Muñoz VM, Acosta-González RI, Plancarte-Sánchez R, Anaya-Reyes M, Fernández Del Valle-Laisequilla C, Reyes-García JG and Jiménez-Andrade JM: Repeated administration of mazindol reduces spontaneous pain-related behaviors without modifying bone density and microarchitecture in a mouse model of complete Freund's adjuvant-induced knee arthritis. J Pain Res 10: 1777-1786, 2017.
37. Chen S, Fang XQ, Zhang JF, Ma Y, Tang XZ, Zhou ZJ, Wang JY, Qin A and Fan SW: Lycorine protects cartilage through suppressing the expression of matrix metalloprotenases in rat chondrocytes and in a mouse osteoarthritis model. Mol Med Rep 14: 3389-3396, 2016.
38. Luo H, Liu L, Zhao JJ, Mi XF, Wang QJ and Yu M: Effects of oxaliplatin on inflammation and intestinal floras in rats with colorectal cancer. Eur Rev Med Pharmacol Sci 24: 10542-10549, 2020.
39. Hao M, Tang Q, Wang B, Li Y, Ding J, Li M, Xie M and Zhu H: Resveratrol suppresses bone cancer pain in rats by attenuating inflammatory responses through the AMPK/Drp1 signaling. Acta Biochim Biophys Sin (Shanghai) 52: 231-240, 2020.
40. Mao Y, Wang C, Tian X, Huang Y, Zhang Y, Wu H, Yang S, Xu K, Liu Y, Zhang W, *et al*: Endoplasmic reticulum stress contributes to nociception via neuroinflammation in a murine bone cancer pain model. Anesthesiology 132: 357-372, 2020.
41. Shi X, Bai H, Wang J, Wang J, Huang L, He M, Zheng X, Duan Z, Chen D, Zhang J, *et al*: Behavioral assessment of sensory, motor, emotion, and cognition in rodent models of intracerebral hemorrhage. Front Neurol 12: 667511, 2021.
42. Chatterjee P, Pedrini S, Stoops E, Goozee K, Villemagne VL, Asih PR, Verberk IMW, Dave P, Taddei K, Sohrabi HR, *et al*: Plasma glial fibrillary acidic protein is elevated in cognitively normal older adults at risk of Alzheimer's disease. Transl Psychiatry 11: 27, 2021.
43. Kelley N, Jeltema D, Duan Y and He Y: The NLRP3 inflammasome: An overview of mechanisms of activation and regulation. Int J Mol Sci 20: 3328, 2019.
44. Lee MJ, Agrahari G, Kim HY, An EJ, Chun KH, Kang H, Kim YS, Bang CW, Tak LJ and Kim TY: Extracellular superoxide dismutase prevents skin aging by promoting collagen production through the activation of AMPK and Nrf2/HO-1 cascades. J Invest Dermatol 141: 2344-2353.e7, 2021.
45. Chen Y, Maejima Y, Shirakabe A, Yamamoto T, Ikeda Y, Sadoshima J and Zhai P: Ser9 phosphorylation of GSK-3β promotes aging in the heart through suppression of autophagy. J Cardiovasc Aging 1: 9, 2021.
46. Yuan L, Liu C, Wan Y, Yan H and Li T: Effect of HDAC2/Inpp5f on neuropathic pain and cognitive function through regulating PI3K/Akt/GSK-3β signal pathway in rats with neuropathic pain. Exp Ther Med 18: 678-684, 2019.
47. Xu W, Zhu M, Yuan S and Yu W: Spinal CXCL5 contributes to nerve injury-induced neuropathic pain via modulating GSK-3β phosphorylation and activity in rats. Neurosci Lett 634: 52-59, 2016.
48. Rashvand M, Danyali S and Manaheji H: The potential role of glycogen synthase kinase-3β in neuropathy-induced apoptosis in spinal cord. Basic Clin Neurosci 11: 15-30, 2020.
49. Peng Z, Zha L, Yang M, Li Y, Guo X and Feng Z: Effects of ghrelin on pGSK-3β and β-catenin expression when protects against neuropathic pain behavior in rats challenged with chronic constriction injury. Sci Rep 9: 14664, 2019.
50. Yang HY, Zhang F, Cheng ML, Wu J, Xie M, Yu LZ, Liu L, Xiong J and Zhu HL: Glycogen synthase kinase-3β inhibition decreases inflammation and relieves cancer induced bone pain via reducing Drp1-mediated mitochondrial damage. J Cell Mol Med 26: 3965-3976, 2022.
51. Shu Z, Miao X, Tang T, Zhan P, Zeng L and Jiang Y: The GSK-3β/β-catenin signaling pathway is involved in HMGB1-induced chondrocyte apoptosis and cartilage matrix degradation. Int J Mol Med 45: 769-778, 2020.
52. Shin D, Lee SC, Heo YS, Lee WY, Cho YS, Kim YE, Hyun YL, Cho JM, Lee YS and Ro S: Design and synthesis of 7-hydroxy-1H-benzoimidazole derivatives as novel inhibitors of glycogen synthase kinase-3beta. Bioorg Med Chem Lett 17: 5686-5689, 2007.
53. Dutta M, Tareq AM, Rakib A, Mahmud S, Sami SA, Mallick J, Islam MN, Majumder M, Uddin MZ, Alsubaie A, *et al*: Phytochemicals from leucas zeylanica targeting main protease of SARS-CoV-2: Chemical profiles, molecular docking, and molecular dynamics simulations. Biology (Basel) 10: 789, 2021.

54. Li H, Zhang W, Lou Q, Chang Y, Lin Z and Lou L: XueFu ZhuYu Decoction alleviates cardiopulmonary bypass-induced NLRP3 inflammasome-dependent pyroptosis by inhibiting IkB-α/NF-κB pathway in acute lung injury rats. Evid Based Complement Alternat Med 2022: 6248870, 2022.
55. Lee KM, Kang BS, Lee HL, Son SJ, Hwang SH, Kim DS, Park JS and Cho HJ: Spinal NF-kB activation induces COX-2 upregulation and contributes to inflammatory pain hypersensitivity. Eur J Neurosci 19: 3375-3381, 2004.
56. Liu J, Sun S, Zhou C, Sun Z, Wang Q and Sun C: In vitro and in vivo anticancer activity of Lycorine in prostate cancer by inhibiting NF-κB signaling pathway. J Cancer 13: 3151-3159, 2022.
57. Ge X, Meng X, Fei D, Kang K, Wang Q and Zhao M: Lycorine attenuates lipopolysaccharide-induced acute lung injury through the HMGB1/TLRs/NF-κB pathway. 3 Biotech 10: 369, 2020.
58. Steinbrecher KA, Wilson W III, Cogswell PC and Baldwin AS: Glycogen synthase kinase 3beta functions to specify gene-specific, NF-kappaB-dependent transcription. Mol Cell Biol 25: 8444-8455, 2005.
59. Medunjanin S, Schleithoff L, Fiegehenn C, Weinert S, Zuschratter W and Braun-Dullaeus RC: GSK-3β controls NF-kappaB activity via IKKγ/NEMO. Sci Rep 6: 38553, 2016.
60. Rada P, Rojo AI, Chowdhry S, McMahon M, Hayes JD and Cuadrado A: SCF/{beta}-TrCP promotes glycogen synthase kinase 3-dependent degradation of the Nrf2 transcription factor in a Keap1-independent manner. Mol Cell Biol 31: 1121-1133, 2011.
61. Chen X, Liu Y, Zhu J, Lei S, Dong Y, Li L, Jiang B, Tan L, Wu J, Yu S and Zhao Y: GSK-3β downregulates Nrf2 in cultured cortical neurons and in a rat model of cerebral ischemia-reperfusion. Sci Rep 6: 20196, 2016.
62. Arendt-Nielsen L, Morlion B, Perrot S, Dahan A, Dickenson A, Kress HG, Wells C, Bouhassira D and Drewes AM: Assessment and manifestation of central sensitisation across different chronic pain conditions. Eur J Pain 22: 216-241, 2018.
63. Lluch E, Nijs J, Courtney CA, Rebbeck T, Wylde V, Baert I, Wideman TH, Howells N and Skou ST: Clinical descriptors for the recognition of central sensitization pain in patients with knee osteoarthritis. Disabil Rehabil 40: 2836-2845, 2018.
64. Pan TT, Pan F, Gao W, Hu SS and and Wang D: Involvement of macrophages and spinal microglia in osteoarthritis pain. Curr Rheumatol Rep 23: 29, 2021.